Desalination and Water Treatment
www.deswater.com

doi: 10.5004/dwt.2017.20735

74 (2017) 44–52
May

Structure and properties of membrane at different ages in drinking water treatment

L. Cui[a], Z. Feng[a], C. Goodwin[b], W. Gao[c], B.Q. Liao[a,*]

[a]*Department of Chemical Engineering, Lakehead University, 955 Oliver Road, Thunder Bay, ON, Canada P7B 5E1, emails: bliao@lakeheadu.ca (B.Q. Liao), lcui@lakeheadu.ca (L. Cui), zfeng1@lakeheadu.ca (Z. Feng)*
[b]*Environmental Division, City of Thunder Bay, Victoriaville Civic Center, Thunder Bay, ON, Canada P7C 5K4, email: cgoodwin@thunderbay.ca*
[c]*Department of Civil Engineering, Lakehead University, 955 Oliver Road, Thunder Bay, ON, Canada P7B 5E1, email: wagao@lakeheadu.ca*

Received 20 November 2016; Accepted 21 March 2017

ABSTRACT

Effects of membrane aging and chemical cleaning on hollow fiber (HF) membrane properties (morphology, permeability, porosity, hydrophilicity, and physical strength) were systematically investigated by using membrane samples at different ages from a full-scale drinking water membrane filtration plant. Scanning electron microscopic images showed that the extent of fouling on membrane surfaces increased and the diameter of HF membrane decreased with membrane age extended. Membrane permeability, porosity, and break strength were also decreased with an increase in membrane age. Dextran rejection results and scanning electron microscope images showed the same trend in a decrease in membrane pore size with the membrane operational time extended. Chemical cleaning studies showed that organic fouling was important fouling mechanism. The membrane permeability, porosity, and hydrophilicity improved after chemical cleaning. The deterioration of membrane performance with an increase in membrane age correlated well with the changes in membrane properties and fouling.

Keywords: Membrane properties; Membrane aging, Membrane structure, Chemical cleaning; Permeability; Surface morphology

1. Introduction

In recent years, membranes have become fully or partially integrated into a number of drinking water production facilities all over the world [1–3]. This is due to the advantages of membrane filtration, such as simplicity, robust operation, superior drinking water quality, easy to scale-up, reduced chemical and energy usages, and to the fact that membrane processes can resolve technically complex and, at times, conflicting requirements related to compliance with multi-contaminant regulations [4,5]. Hollow fiber (HF) membranes are widely used in many applications because of its higher packing density and readily permit backwashing. The pore sizes of microfiltration (MF) and ultrafiltration (UF) membranes are in the range from 0.05 to 5 μm and from 1 to 50 nm, respectively [6].

UF membranes have been widely used in drinking water treatment due to their low cost and the fact that they can be easily maintained [7,8]. UF is a process of separating small suspended particles and dissolved macromolecules from fluids using asymmetric membranes. The primary basis of separation is molecular size although secondary factors such as molecular shape and charge can play a significant role as well [9]. UF membranes are often operated in a tangential flow mode where the feed stream sweeps tangentially across the upstream surface of membranes as filtration occurs, thereby maximizing flux rates and membrane life.

---

[*] Corresponding author.

1944-3994/1944-3986

Membrane aging has received much attention in recent year, due to its impact on membrane performance and membrane properties [10–12]. In a full-scale plant, membrane aging could be caused by fouling, chemical cleaning, seasonal change in raw water temperature, and operating conditions (sucking and backwashing mechanical forces) [13–15], while in lab-scale studies, factors that cause membrane aging were isolated and investigated. He et al. [16] investigated the effect of membrane aging on the properties and performance of UF membranes in potable water treatment. It was revealed that aging played a significant role in the deterioration of the tensile strength of the membrane media, as well as the degradation of the intensity of surface resident functional groups, which led to the accumulation of foulants. Bogati et al. [17] studied the effect of chemical cleaning on membrane properties. They showed that under the same dose, a lower concentration combined with a longer soak time could achieve a higher permeability recovery. Meanwhile, a lower pH was more effective in permeability recovery than a higher concentration of citric acid.

Literature review showed that there were limited studies focusing on the effect of membrane aging on membrane structure (porosity and membrane diameter) from full-scale plant membrane samples. The purpose of this study was to investigate the effect of aging under seasonal temperature change on membrane properties and chemical cleaning performance by harvesting membrane samples from a long-term full-scale potable water membrane filtration plant. For this, five HF membranes at different ages were obtained from a drinking water membrane filtration plant to evaluate the changes in membrane structure and properties.

2. Materials and methods

2.1. Materials

The HF membranes with different aging times (new membrane: 0.8, 1.5, 1.8, and 2.5 years old) used in this study were harvested from a full-scale drinking water membrane filtration plant in Northern Ontario, Canada. The plant uses polyvinylidene fluoride (PVDF) HF membranes for drinking water production. The PVDF membrane has a nominal pore size of 0.024 μm. The membranes are operated at a membrane flux of 15–35 L/m^2 h (LMH). One operational cycle includes 240–360 min permeation (93% recovery) and 300 s backwashing. The cleaning strategies include both maintenance cleans (seven hypochlorite cleanings at 100 mg/L per week) and recovery cleans (12 hypochlorite cleanings at 500 mg/L per year and 6 citric acid cleaning at 2,000 mg/L per year). The raw water characteristics are summarized in our previous publications [16,17].

2.2. Membrane bundles

Nine pieces of outside-in flow path HF membrane with approximately 23 cm effective length of each fiber were sealed to make a lab-scale membrane bundle with a total effective membrane area of about 6.18×10^{-3} m^2. The nine pieces of HF were glued together by using epoxy resin. After the glue became dry, a plastic sleeve was put on. Two membrane bundles were made for each membrane sample for duplicate experiments. The prepared membrane bundles were immersed in deionized water for further use.

2.3. Membrane cleaning

Some of the fouled membrane bundles were cleaned by chemical methods, in order to study the effect of chemical cleaning on membrane properties (before vs. after chemical cleaning). First, the membrane bundle was soaked in sodium hypochlorite (NaClO; Product No.: 239305, Sigma-Aldrich, Oakville, ON, Canada) solution with the concentration of 200 ppm for 2 h; then immersed by 2,000 ppm of citric acid (Product No.: 251275, Sigma-Aldrich) solution for another 2 h; finally, the membrane bundle was washed thoroughly by deionized water for removing the chemicals. The choice of chemical cleaning conditions was based on the suggestions of the membrane supplier and the results of our previous studies on optimization of chemical cleanings [16,17].

2.4. Membrane morphology observation

Membrane morphology was examined using a scanning electron microscope (SEM; SU70, Hitachi, Japan). To preserve membrane structure with minimum changes, drying of wet membrane samples was conducted by liquid nitrogen. A piece of wet membrane fiber was immersed in liquid nitrogen for about 10 min, then the membrane was carefully cut by a blade to maintain the structure and integrity, such as the cross-sectional areas of membrane samples, from damage of cutting [18]. The specimen was coated with gold for cross-section observation and carbon for outer and inner surface observation by a sputter coater (Model 12560, Fullam, USA). Samples were observed under an electron microscope at 10 kV. The diameter of lumen and thickness of membrane from cross-section images were measured by the software of ImageJ (Version 1.51d, National Institutes of Health, USA).

2.5. Pore size distribution

The membrane pore size distribution was determined by using the membrane outer surface SEM photomicrographs. Membrane pore size and distribution percentage were calculated by the Nano Measurer software (Version 1.2.5, Fudan University, China).

2.6. Permeability

The membrane permeability was measured by using a simple dead-end filtration setup. The membrane bundle was placed in a beaker with deionized water. The transmembrane pressure (TMP) was gradually increased by adjusting the speed of permeation pump and the corresponding water flux was measured. The water permeation flux was measured at the room temperature of 21°C ± 1°C. The permeability of the membranes was calculated by using the following Eq. (1) [19]:

$$P = \frac{J}{\Delta P \times A} = \frac{J}{n\pi D l \Delta P} \tag{1}$$

where P is the specific permeability of the HF membrane (LMH/bar); J is the pure water flux (L/h); ΔP is the pressure difference between the feed side and the permeation side of the membrane (bar); A is the effective membrane surface area (m^2); n is the number of fibers in the bundle; D is the outer diameter of HF (m); and l represents the effective length of HF (m).

2.7. Dextran rejection determination

Dextran rejection tests were performed using a dextran (Product No.: 31425, Sigma-Aldrich) with specific molecular weight of 670 kDa. This dextran (670 kDa) was selected to give a retention of around 80%, based on the results of a test series of dextran with lower molecular weights. Dextran solutions of 60 mg/L were prepared by dissolving pre-weighted amounts of dextran in deionized distilled water. The selection of 670 kDa dextran was most suitable dextran for pore size characterization, based on the availability of high molecular weights dextran and preliminary studies with different molecular weight dextran. The concentrations of the feed and permeate were analyzed with a spectrophotometer (DR 2800, Hach, USA) at 625 nm according to Gaudy [20].

The dextran rejection (R) is defined as:

$$R = \left(1 - \frac{C_p}{C_f}\right) \times 100\% \tag{2}$$

where C_f and C_p represent the solute concentration in the feed and permeate solutions, respectively [19].

2.8. Porosity

Gravimetric method was used for assessing the porosity which calculated the weight of liquid immersed in the membrane pores. The specific length of membrane sample was immersed in the deionized water for at least 24 h. Then the water absorbed on the outer membrane surface was removed by a filter paper. After that, wet membrane's weight was measured and the dry membrane's weight was measured after drying in an oven overnight at the temperature of 105°C. The membrane overall porosity (Ɛ) was calculated by the following Eq. (3) [21]:

$$\varepsilon = \frac{V_{\text{water}}}{V_{\text{membrane}}} = \frac{\dfrac{W_1 - W_2 - W_3}{\rho}}{\left(\dfrac{\pi}{4}\right)\left(D^2 - d^2\right)l} \times 100\% \tag{3}$$

where D is the outer diameter (mm), d is the inner diameter (mm), l is the length of sample membrane (mm), ρ is the density of deionized water (1.0 g/cm^3), W_1 is the weight of wet membrane (g), W_2 is the weight of dry membrane (g), and W_3 is the weight of water in membrane hollow section (g).

$$W_3 = \frac{\pi d^2 l \rho}{4} \tag{4}$$

2.9. Hydrophilicity

The water contact angle of the membrane surface was measured by using the sessile drop method, and all the contact angle data were an average of 10 measurements on different locations of the membrane surface. A water drop was dripped on the outer surface of HF membrane. After 10 s when the droplet was stable on the outer surface, the projected drop image was determined by the optical contact angle meter (Theta Lite 100, Biolin Scientific, USA) at room temperature [21]. The contact angle results were analyzed by OneAttension software (Version 2.5, Biolin Scientific, USA).

2.10. Break strength

The break strength of the HF membranes was measured by using a dual-range force sensor (Au Physics Enterprises, MI, USA) at room temperature. The membrane samples were cut into about 10 cm long segments, and then knotted onto the hook of the sensor. With pulling manually, the tensile strength at the break point of the HF membrane was recorded by a Data-Collection Software (Logger Pro 3, Vernier Software & Technology, USA). The break strength (MPa) of the membrane was calculated by using tensile strength at the break point (N) divided by the cross-section area of membrane (m^2).

2.11. Statistical analysis

All statistical analyses were conducted using the single factor analysis of variance (ANOVA) in Microsoft Excel 2016. ANOVA was employed to test for differences among treatment methods, when studying the influence of membrane aging on membrane properties. The p value was set at 0.05 for all statistical testing performed in this study.

3. Results

3.1. Membrane morphology

The SEM micrographs of cross-section, inner surface, and outer surface of the membranes were taken at various magnifications to study the membrane morphology.

All the membranes used in this study have a thin skin layer and the finger-like structure extends from the outer surface to the inner surface with the sponge-like structure as shown in Fig. 1(a). The membrane cross-section images show there is no visible difference for the new membrane and the different aged membranes. Furthermore, all the membrane showed the loose structure in their inner surface as shown in Fig. 1(b).

For the HF membrane samples without any cleaning, the results in Table 1 indicate that with the increase of membrane age, the diameter of membrane lumen decreased from 508.91 μm for new membrane to 466.34 μm for 2.5-year-old membrane (ANOVA, $p < 0.05$). Meanwhile, the thickness of membrane did not show significant differences for different membranes, which ranged between 225.02 and 233.79 μm (ANOVA, $p > 0.05$).

When the chemical cleaning applied to the aged membrane, the results in Table 1 show that both diameter of membrane lumen and membrane thickness did not appear any

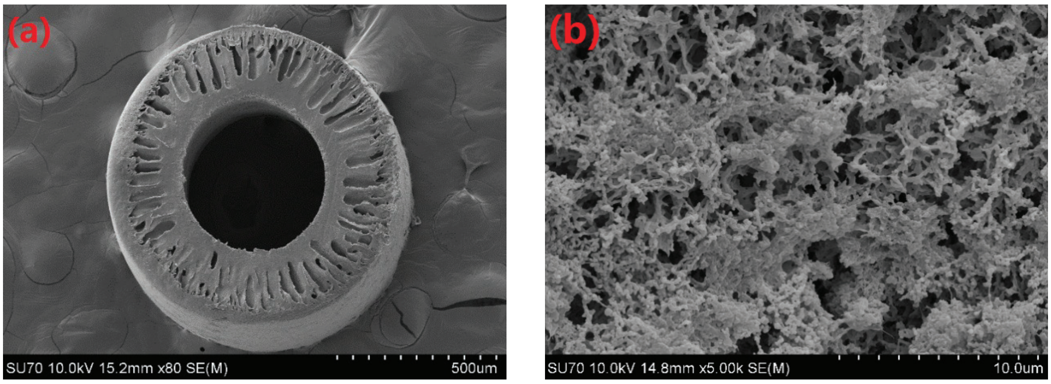

Fig. 1. Cross-section (a) and inner surface (b) images of membrane.

Table 1
Membrane cross-section dimensions (μm)

	New	0.8 year old		1.5 years old		1.8 years old		2.5 years old	
		BC[a]	AC[b]	BC	AC	BC	AC	BC	AC
Lumen diameter	508.91	487.23	491.02	483.73	483.71	480.73	474.42	466.34	470.99
	(8.19)[c]	(11.36)	(10.49)	(9.15)	(9.08)	(9.89)	(10.97)	(13.20)	(9.50)
Membrane thickness	225.02	228.28	232.73	233.79	233.66	233.39	230.63	229.66	223.65
	(8.26)	(5.37)	(4.07)	(6.82)	(4.92)	(5.40)	(6.74)	(7.81)	(3.54)

[a] Before two-step cleaning.
[b] After two-step cleaning.
[c] Numbers in brackets are standard deviations.

change compared with the corresponding membranes before chemical cleaning.

Fig. 2 shows the outer surface of different HF membranes before and after two-step chemical cleaning. A number of pores could be observed on the outer surface of the new membrane. For 0.8- and 1.5-year-old membrane, fewer pores were found due to membrane fouling. For 1.8- and 2.5-year-old membrane, there were almost no visible pores left on the outer surface, which indicated that the pores were blocked by foulants, and the membrane surface was also covered by foulants to a certain extent. The membrane outer surface morphology clearly shows that more pores could be observed for 0.8-, 1.5-, and 1.8-year-old membranes after chemical cleaning. For 2.5-year-old membrane, the outer surface became smoother although still no pores could be seen, which was mainly because only the outermost foulant was removed by chemical cleaning. Note that more smooth surfaces were also observed for the other membranes after chemical cleaning for the same reason.

3.2. Pore size distribution

Fig. 3 shows the pore size distribution of membranes from the plant based on increasing operational time. The new membrane has a pore size range from 4.0 to 25.0 nm but majority of the membrane pores are in the range between 12.4 and 14.5 nm, with a frequency of 26.67%. At 0.8 year old, the pores mostly concentrated in the ranges of 9.4 and 11.2 nm before chemical cleaning, while the pores mostly located in the range of 10.3 and 12.4 nm for the membrane after cleaning. At 1.5 years old, the same trend was observed as that of the membrane at 0.8 year old, the pore size decreased and concentration range changed from 5.3 to 9.2 nm for the membrane before cleaning to 10.4–12.0 nm after cleaning. Due to serious fouling of the 1.8- and 2.5-year-old membrane, the pores could not be observed on their outer surface from SEM microphotographs. Therefore, the pore size distribution cannot be calculated before chemical cleaning. However, the membrane at 1.8 years old after chemical cleaning showed the membrane pores mostly distributed within the range of 10.5 and 11.4 nm. For the membrane at 2.5 years old, the applied chemical cleanings were not very effective to recover the pores. For the new membrane and at 0.8 year old, some pores with a size large than 18 nm were observed, while no pores large than 18 nm were observed for the 1.5-, 1.8-, and 2.5-year-old membranes. The results showed that the pore sizes of membrane decreased with an increase in membrane operational time.

3.3. Permeability

The permeability for different HF membranes before and after chemical cleaning is presented in Fig. 4. The permeability had an obvious decrease from new membrane to 1.8-year-old membrane (from 478 to 274.3 LMH/bar) without any cleaning, which decreased 42.62% when compared with the new membrane. From 1.8 to 2.5 years old, there was a distinct drop for permeability from 274.3 to 18.3 LMH/bar, which decreased 93.33%.

Fig. 4 also revealed that NaClO cleaning had a positive effect on membrane permeability recovery. After NaClO cleaning, the permeability recovered by 4.02%, 7.69%, and

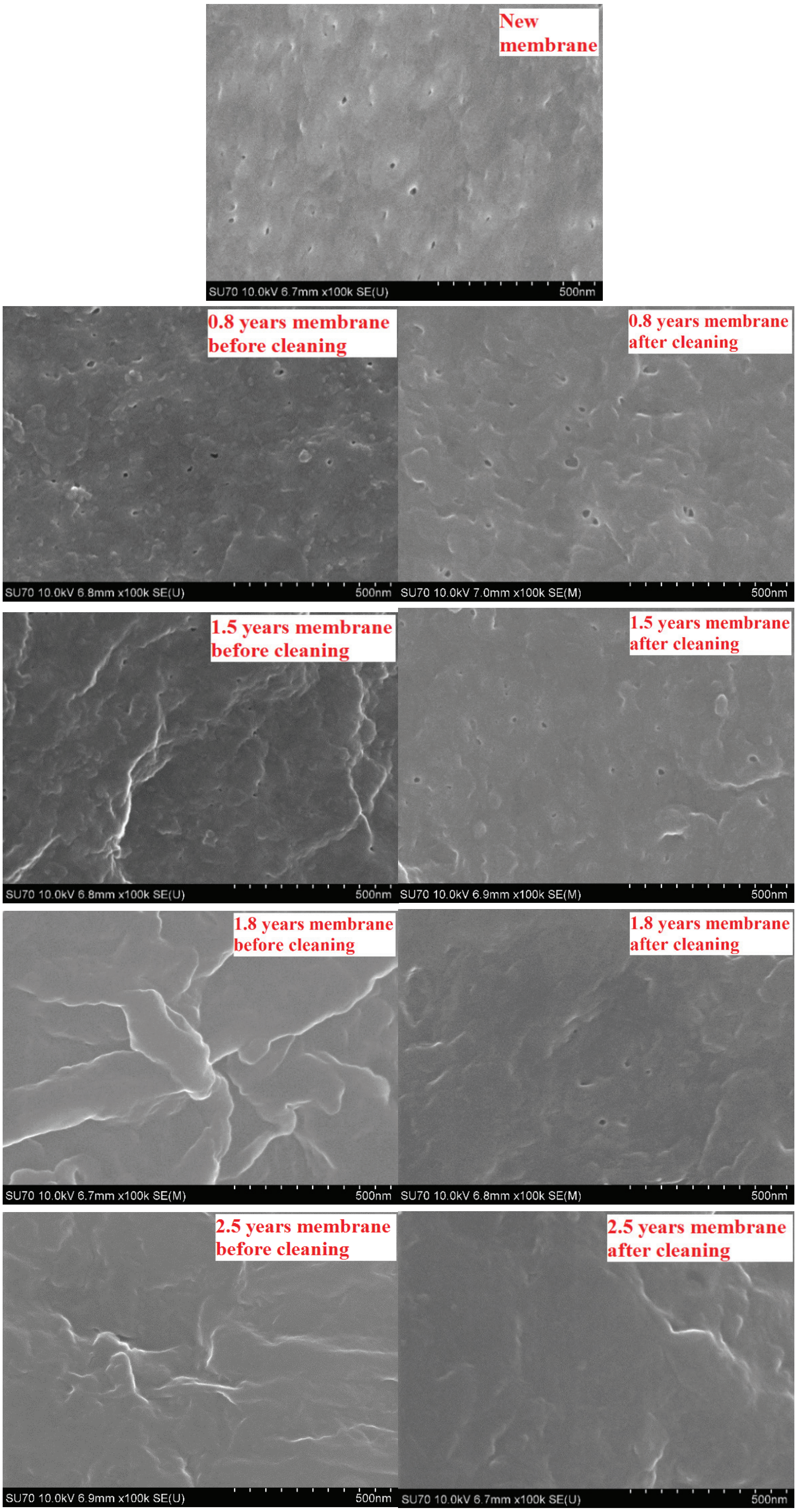

Fig. 2. SEM pictures of outer surface for different membranes.

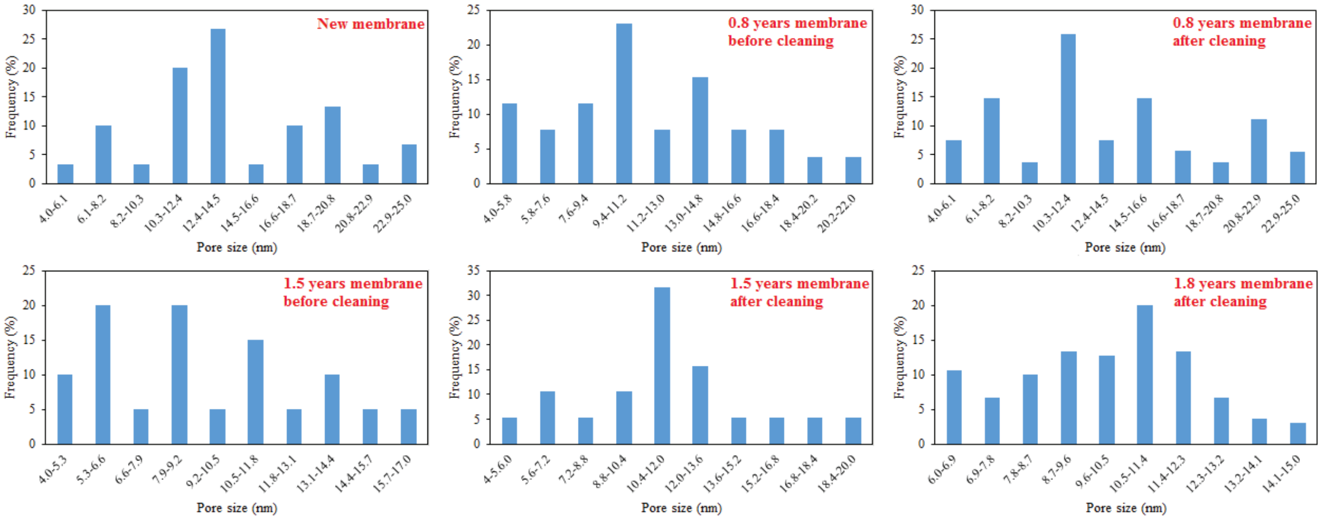

Fig. 3. Pore size distribution of different membranes.

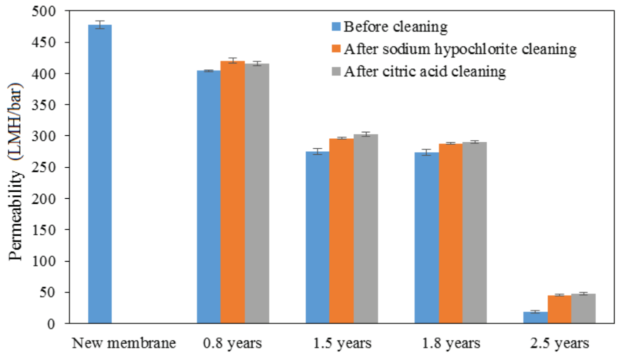

Fig. 4. Pure water permeability of membranes.

5.00% for 0.8-, 1.5-, and 1.8-year-old membranes, respectively, due to the removal of organic foulants. For 2.5-year-old membrane, its permeability increased 146.23% because of its very low initial permeability, as confirmed by the SEM images (there were almost no pores left on the outer surface of membrane).

However, the permeability recovery is significantly lower after citric acid cleaning (ANOVA, $p > 0.05$), which means that inorganic fouling was not a dominant foulant or citric acid cleaning was not effective under tested conditions. Thus, a systematic study on the removal of inorganic foulants, particularly for the 2.5-year-old membrane, should be conducted in future to identify suitable cleaning strategies and recover membrane permeability.

3.4. Dextran rejection

Quantification of rejection properties is very important when comparing performance of membranes with small pores such as UF membranes, since small deviations in pore size can translate into significantly different rejection capabilities for solutes of interest [22].

As shown in Fig. 5, the dextran rejection of new membrane is 81.54%. The dextran rejection of aged membrane without any chemical cleaning increased with the extension of aging time. This was due to the pores on the membrane surface were blocked during filtration process, resulted much more rejection of dextran solutes. The dextran rejections were 83.65%, 85.37%, 89.28%, and 92.16% for 0.8, 1.5-, 1.8-, and 2.5-year-old membrane, respectively (ANOVA, $p < 0.05$). As shown in section 3.2, the main foulants on the membrane surface were organic matters, so after NaClO cleaning, the dextran rejection appeared decrease for all of the used membrane due to the foulant removal, which decreased 3.14%, 2.06%, 5.72%, and 6.46% for 0.8-, 1.5-, 1.8-, and 2.5-year-old membrane (ANOVA, $p < 0.05$), respectively. Citric acid cleaning had smaller impact on membrane dextran rejection.

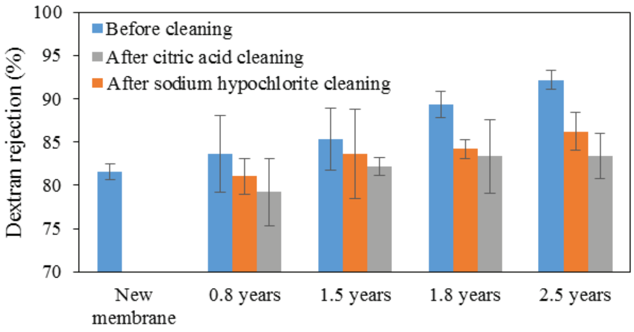

Fig. 5. Dextran rejection of membranes.

3.5. Porosity

Membrane porosity is a criterion of free spaces in the membrane. The higher the membrane porosity, the larger the mass flux through the membrane. As shown in Fig. 6, the membrane porosity decreased from 77.34% for new membrane to 60.88% for 2.5-year-old membrane before chemical cleaning, which was mainly because of membrane fouling (ANOVA, $p < 0.05$). The membrane pores were filled by the foulant, which resulted in a decrease in membrane permeability. The porosity also showed a decreasing trend with an increase in membrane age. After NaClO and citric acid cleaning, the porosity increased slightly when compared with the uncleaned membrane, which was due to the removal of foulant by the chemical cleaning.

3.6. Hydrophilicity

Contact angle measurements are widely used to quantify membrane hydrophobicity. A larger contact angle indicates lower wetting and higher membrane hydrophobicity. The contact angles of all the membranes used in this study were lower than 90°, indicating that they were all hydrophilic in nature and likely to absorb water. As shown in Fig. 7, the new membrane shows hydrophilic which is due to the material (PVDF) itself. The contact angle dropped from 72.9° measured on new membrane to 62.88° measured on 1.8-year-old membrane without chemical cleaning (ANOVA, $p < 0.05$), then insignificant change showed for 2.5-year-old membrane (ANOVA, $p > 0.05$). Afterwards, the contact angle for each membrane after chemical cleaning continuously dropped with different extends. The increased membrane hydrophilicity after NaClO cleaning is reported and explained by surface modification by foulant, cleaning agents, or both [23,24]. Levitsky et al. [25] proposed that the partial scission of membrane polymers increased the surface charge and the more charged membrane became more hydrophilic. The PVDF is a chlorine resistant polymer, and hydrophilization of used membrane is related to the gradual elimination of the surface preservation residues [26,27].

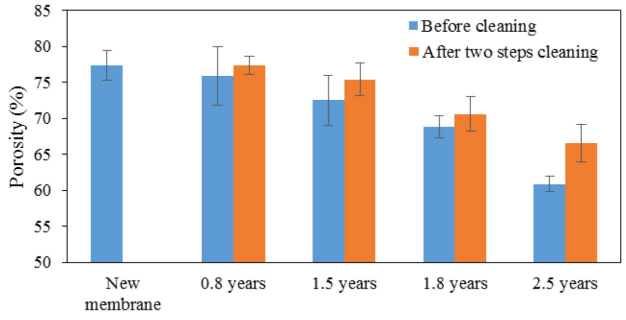

Fig. 6. Porosity of membranes.

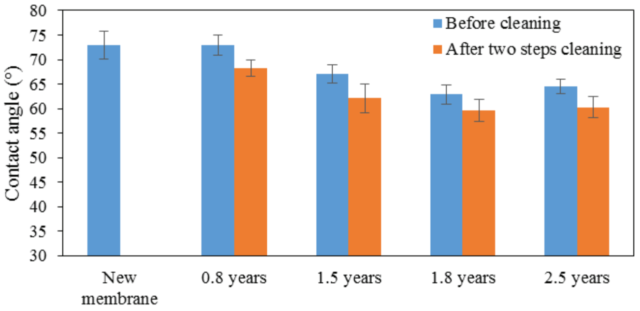

Fig. 7. Contact angle of membranes.

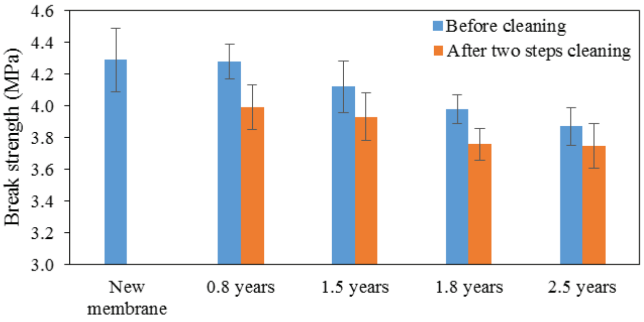

Fig. 8. Break strength of membranes.

3.7. Break strength

Break strength is typically utilized to evaluate the mechanical property of a membrane, and it is very important in field applications. The impacts of membrane fouling on the mechanical properties of membranes remains actively debated, though it might be deduced that this attribute is altered due to repeated backwashing and chemical cleaning [16]. As shown in Fig. 8, without any chemical cleaning, the break strength of membrane had a decreasing trend with an increase in membrane age, which decreased from 4.29 MPa for new membrane to 3.87 MPa for 2.5-year-old membrane (ANOVA, $p < 0.05$). Note that after two-step chemical cleaning, the break strength showed a slightly decrease for different membranes. This result indicates the membrane became more brittle, various functional groups such as aldehyde (CHO), carboxyl (COOH), and ketone (C=O) could be oxidized by exposure to NaClO (oxidant) solution, which resulted the gradual degradation in the mechanical properties of membranes after chemical cleaning [17].

4. Discussion

During HF membrane filtration process, colloidal particles, and large molecular weight natural organic matters (NOMs) are accumulated in the concentrate boundary layer next to the membrane surface and some are attached on membrane surfaces forming a fouling layer. Figs. 1 and 2 clearly showed that the outer surfaces were covered by foulants, while the inner surfaces were clean with no visible fouling. That is because the outer surfaces were in direct contact with colloidal particles and NOM, while the inner surfaces were in contact with permeate (Fig. 2). There were no significant differences on membrane cross-section and inner surface for different aged membranes (Fig. 1). The important finding on the decreased lumen diameter of HF UF with membrane age might be related to the seasonal temperature change, the cold winter raw water temperature (0.3°C–0.4°C) could cause the shrinkage of HF UF and thus led to a decrease in the lumen diameter with the extension of membrane aging time (Table 1). However, the thickness of membrane did not show obvious change. Furthermore, chemical cleaning might contribute to the decrease in HF membrane lumen diameters as well. Thus, the real cause of HF membrane lumen diameter with membrane aging should be identified under well-controlled conditions.

The permeability of membranes decreased with an increase in membrane age (Fig. 4). This is well correlated to the changes in the extent of membrane fouling (Figs. 2 and 3). Furthermore, the decrease in permeability could be at least partially attributed to changes in membrane structure (Table 1 and Figs. 1–3, 5 and 6) at different ages. The decrease in pore size (Fig. 5), porosity (Fig. 6), lumen diameter (Table 1) with an increase in membrane age would be related to an increase in the hydraulic resistance or TMP and thus decreased permeability. The pure water permeability for the different aged membranes after NaClO cleaning showed an increase, due to some foulant removal from membrane outer surfaces (Fig. 4). Liu et al. [28] reported that organic fouling is profound in membrane filtration with source water containing a relatively high level of NOMs. Surface water (lake, river) typically contains a higher level of NOMs than groundwater, with exceptions. For source water with a high level of NOM, organic fouling is believed to be the most significant factor contributing to permeability decline. Furthermore, the internal pore plugging would cause greater hydraulic resistance than cake formed on membrane surface [29]. This is intriguing when one considers the fouling caused by NOM. Because most of NOM have sizes less than pore diameters of MF and UF used in drinking water filtration, adsorption of NOMs on the membrane is a plausible mechanism. It also has been reported that pores appeared to be more preferable sites for adsorption [30]. The explanations above may exhibit why organic fouling typically causes membrane flux decline. Fig. 2 appears to demonstrate that surface fouling is the primary mechanism in these membranes. This seems confirmed in Fig. 5 as after two-step cleaning the pore size is partially restored although permeability is not. Therefore, surface fouling may be the dominant fouling mechanism. On the other hand, citric acid cleaning showed no obvious effect on permeability recovery in this study (Fig. 4). This might suggest citric acid, as a chelating agent for Fe, was not effective in dissolving inorganic foulants containing Ca, Mg, Si, S, etc. The pH level was more important than the citric acid concentration in removing inorganic foulants [17]. Further studies on inorganic foulants removal, particularly for the 2.5-year-old membrane, should focus on the use of different inorganic acids, like H_3PO_4, HNO_3, HCl, or H_2SO_4, at a lower pH or the use of ultrasonic method.

The increased dextran rejection results for aged membranes were due to membrane pores blocked with the extension of membrane operation time (Fig. 5). The decreased membrane pore sizes, as suggested by Fig. 5, could be explained by membrane fouling (Figs. 2 and 3) and decreased membrane porosity (Fig. 6) caused by membrane shrinkage at cold temperature (0.3°C–0.4°C). Noteworthily, even if the pores were not blocked by foulant entirely, the size of pores might be reduced due to the accumulation of foulants inside the pores when compared with the new membrane. This might also explain why the dextran retention increased with an increase in membrane age. The membrane pore size partially restored (with foulant removal) after NaClO cleaning to aged membrane, the dextran retention decreased (pore sizes increased) for all the membranes. Because of citric acid was not effective on foulant removal, the dextran rejection did not show significant change after citric acid cleaning.

The porosity of membrane decreased with an increase in membrane age. This could be caused by membrane fouling on the membrane outer surface (Fig. 2) and decreased membrane internal pore sizes (Fig. 5). For 1.5-year-old membrane, the porosity was just 4.85% lower than that of new membrane, which was due to only part of membrane surface was covered by foulant (Fig. 2). However, there were no visible pores observed on the outer surface of 2.5-year-old membrane, which might also cause partially internal pore plugging, resulted in a significant decrease (16.46%) in porosity as compared with that of the new membrane. Furthermore, the porosity of all the membranes increased after chemical cleaning due to the foulants removal.

Fig. 7 shows the contact angle decreased with the extension of aging time, which means the aged membrane tended to be more hydrophilic. The increase in hydrophilicity would be due to the presence of polar foulants attached on the membrane outer surfaces at different membrane ages. After chemical cleaning, the contact angles for all the membranes showed a decreasing trend. It could be concluded that as more hydrophilic sites (i.e., polar groups) were exposed on the membrane surface when NaClO and citric acid were applied to membrane as cleaning reagents [11].

In general, tensile strength is negatively impacted by aging. This was due to the fact that membranes became less robust with ageing, so had the potential break or breach more frequently. It has been suggested that the decline in mechanical properties indicates a propensity for fiber breakage [31]. Thus, the membrane configuration should be considered in correlating mechanical properties to membrane breaches. The results in Fig. 8 reveal that the deterioration of break strength of aged membranes over time with the interesting result of measureable loss of tensile strength over just one clean set, which had a good agreement with the findings of He et al. [16]. In addition, the decrease of tensile strength after chemical cleaning may be due to modification of membrane surface chemistry, the membrane surface deteriorated as demonstrated by the decreasing intensity of functional groups (CH, CH_2, and C=O) [32].

5. Conclusions

The study of HF UF membranes from a long-term operational full-scale drinking water membrane filtration plant at different ages suggests the following conclusions:

- With the extension of aging time, more pores on the membrane surface were blocked by foulants. Chemical cleaning with NaClO solution followed by citric acid could partially restore membrane permeability.
- The diameter of membrane lumen, membrane porosity, and membrane pore sizes decreased with an increase in membrane ages. These changes could be related to the accumulation of membrane foulants and potentially cold temperature effect.
- The decrease in membrane permeability correlated well with the changes in membrane structure with an increase in membrane age.
- Chemical cleaning could partially restore membrane permeability and porosity, but had negative effect on membrane break strength.
- Membrane hydrophilicity increased with an increase in membrane age and after chemical cleaning. This could be attributed to membrane polymers deterioration and surface preservation residues elimination.

Acknowledgment

The authors are thankful for the financial support of the Natural Science and Engineering Research Council of Canada (NSERC).

References

[1] F. Chen, S. Peldszus, R.H. Peiris, A.S. Ruhl, R. Mehrez, M. Jekel, R.L. Legge, P.M. Huck, Pilot-scale investigation of drinking water ultrafiltration membrane fouling rates using advanced data analysis techniques, Water Res., 48 (2014) 508–518.

[2] S. Metsämuuronen, M. Sillanpää, A. Bhatnagar, M. Mänttäri, Natural organic matter removal from drinking water by membrane technology, Sep. Purif. Rev., 43 (2014) 1–61.

[3] R.H. Peiris, M. Jaklewicz, H. Budman, R.L. Legge, C. Moresoli, Assessing the role of feed water constituents in irreversible membrane fouling of pilot-scale ultrafiltration drinking water treatment systems, Water Res., 47 (2013) 3364–3374.

[4] R.L. Han, J.H. Zeng, L. Han, Y.Q. Wang, Q.B. Chang, X.Z. Zhang, J. Zhou, Application of integrated membrane technology in purification of chlorogenic acid, Desal. Wat. Treat., 55 (2015) 2165–2170.

[5] D. Norberg, S. Hong, J. Taylor, Y. Zhao, Surface characterization and performance evaluation of commercial fouling resistant low-pressure RO membranes, Desalination, 202 (2007) 45–52.

[6] E. Akhondi, F. Wicaksana, W.B. Krantz, A.G. Fane, Evapoporometry determination of pore-size distribution and pore fouling of hollow fiber membranes, J. Membr. Sci., 470 (2014) 334–345.

[7] P. Shen, A. Moriya, S. Rajabzadeh, T. Maruyama, H. Matsuyama, Improvement of the antifouling properties of poly (lactic acid) hollow fiber membranes with poly (lactic acid)-polyethylene glycol-poly (lactic acid) copolymers, Desalination, 325 (2013) 37–39.

[8] J.L. Soler-Cabezas, M. Torà-Grau, M.C. Vincent-Vela, J.A. Mendoza-Roca, F.J. Martínez-Francisco, Ultrafiltration of municipal wastewater: study on fouling models and fouling mechanisms, Desal. Wat. Treat., 56 (2015) 3427–3437.

[9] B.K. Chaturvedi, A.K. Ghosh, V. Ramachandhran, M.K. Trivedi, M.S. Hanra, B.M. Misra, Preparation, characterization and performance of polyethersulfone ultrafiltration membranes, Desalination, 133 (2001) 31–40.

[10] F. Liu, N.A. Hashim, Y. Liu, M.R.M. Abed, K. Li, Progress in the production and modification of PVDF membranes, J. Membr. Sci., 375 (2011) 1–27.

[11] J. Ravereau, A. Fabre, A. Brehant, R. Bonnard, C. Sollogoub, J. Verdu, Ageing of polyvinylidene fluoride hollow fiber membranes in sodium hypochlorite solutions, J. Membr. Sci., 505 (2016) 174–184.

[12] A. Touffet, J. Baron, B. Welte, M. Joyeux, B. Teychene, H. Gallard, Impact of pretreatment conditions and chemical ageing on ultrafiltration membrane performances. Diagnostic of a coagulation/adsorption/filtration process, J. Membr. Sci., 489 (2015) 284–291.

[13] E. Akhondi, F. Wicaksana, A.G. Fane, Evaluation of fouling deposition, fouling reversibility and energy consumption of submerged hollow fiber membrane systems with periodic backwash, J. Membr. Sci., 452 (2014) 319–331.

[14] T. Zsirai, P. Buzatu, P. Aerts, S. Judd, Efficacy of relaxation, backflushing, chemical cleaning and clogging removal for an immersed hollow fiber membrane bioreactor, Water Res., 46 (2012) 4499–4507.

[15] H. Norafifah, M.Y. Noordin, K.Y. Wong, S. Izman, A.N.A. Ahmad, A study of operational factors for reducing the fouling of hollow fiber membranes during wastewater filtration, Procedia CIRP, 26 (2015) 781–785.

[16] Y. He, J. Sharma, R. Bogati, B.Q. Liao, C. Goodwin, K. Marshall, Impacts of aging and chemical cleaning on the properties and performance of ultrafiltration membranes in potable water treatment, Sep. Sci. Technol., 49 (2014) 1317–1325.

[17] R. Bogati, C. Goodwin, K. Marshall, K.T. Leung, B.Q. Liao, Optimization of chemical cleaning for improvement of membrane performance and fouling control in drinking water treatment, Sep. Sci. Technol., 50 (2015) 1835–1845.

[18] B.F.K. Kingsbury, K. Li, A morphology study of ceramic hollow fiber membranes, J. Membr. Sci., 328 (2009) 134–140.

[19] R. Wang, L. Shi, C.Y. Tang, S.R. Chou, C.Q. Qiu, A.G. Fane, Characterization of novel forward osmosis hollow fiber membranes, J. Membr. Sci., 355 (2010) 158–167.

[20] A.F. Gaudy, Colorimetric determination of protein and carbohydrate, Ind. Water Waste, 7 (1962) 17–22.

[21] K.K. Chen, C.F. Xiao, Q.L. Huang, H. Liu, H.L. Liu, Y.J. Wu, Z. Liu, Study on vacuum membrane distillation (VMD) using FEP hollow fiber membrane, Desalination, 375 (2015) 24–32.

[22] B.S. Lalia, V. Kochkodan, R. Hashaikeh, N. Hilal, A review on membrane fabrication: structure, properties and performance relationship, Desalination, 326(2013) 77–95.

[23] P. Wang, Z.W. Wang, Z.C. Wu, Q. Zhou, D.H. Yang, Effect of hypochlorite cleaning on the physiochemical characteristics of polyvinylidene fluoride membranes, Chem. Eng. J., 162 (2010) 1050–1056.

[24] V. Puspitasari, A. Granville, P. Le-Clech, V. Chen, Cleaning and aging effect of sodium hypochlorite on polyvinylidene fluoride (PVDF) membranes, Sep. Purif. Technol., 72 (2010) 301–308.

[25] I. Levitsky, A. Duek, E. Arkhangelsky, D. Pinchev, T. Kadoshian, H. Shetrit, R. Naim, V. Gitis, Understanding the oxidative cleaning of UF membranes, J. Membr. Sci., 377 (2011) 206–213.

[26] M. Momtaz, J.L. Dewez, J. Marchand-Brynaert, Chemical reactivity assay and surface characterization of a poly(vinylidene fluoride) microfiltration membrane (“Durapore DVPP”), J. Membr. Sci., 250 (2005) 29–37.

[27] E. Arkhangelsky, I. Levitsky, V. Gitis, Electrostatic repulsion as a mechanism in fouling of ultrafiltration membranes, Water Sci. Technol., 58 (2008) 1955–1961.

[28] C. Liu, S. Caothien, J. Hayes, T. Caothuy, T. Otoyo, T. Ogawa, Membrane Chemical Cleaning: From Art to Science, Proc. 2001 Membrane Technology Conference, AWWA, 2001, pp. 1–25.

[29] H.Q. Chang, F.S. Qu, H. Liang, R.B. Jia, H.R. Yu, S.L. Shao, K. Li, W. Gao, G.B. Li, Correlating ultrafiltration membrane fouling with membrane properties, water quality, and permeate flux, Desal. Wat. Treat., 56 (2015) 1746–1757.

[30] C. Jucker, M.M. Clark, Adsorption of aquatic humic substances on hydrophobic ultrafiltration membranes, J. Membr. Sci., 97 (1994) 37–52.

[31] S. Robinson, S.Z. Abdullah, P. Bérubé, P. Le-Clech, Ageing of membranes for water treatment: Linking changes to performance, J. Membr. Sci., 503 (2016) 177–187.

[32] R. Bogati, Membrane Fouling and Its Control in Drinking Water Membrane Filtration Process, MSc Thesis, Department of Chemical Engineering, Lakehead University, Thunder Bay, ON, Canada, 2013.